Send Orders for Reprints to reprints@benthamscience.net

Current Computer-Aided Drug Design, 2021, *17*, 57-68

RESEARCH ARTICLE

Identification of Novel Cyclin A2 Binding site and Nanomolar Inhibitors of Cyclin A2-CDK2 Complex

Stephanie S. Kim[1,#], Michele Joana Alves[2,#], Patrick Gygli[2], Jose Otero[2,*] and Steffen Lindert[1,*]

[1]*Department of Chemistry and Biochemistry, Ohio State University, Columbus, OH, 43210, USA;* [2]*Departments of Neuroscience, Pathology, Neuropathology, Ohio State University, Columbus, OH, 43210, USA*

ARTICLE HISTORY

Received: August 19, 2019
Revised: November 25, 2019
Accepted: December 09, 2019

DOI:
10.2174/1573409916666191231113055

Abstract: ***Background*:** Given the diverse roles of cyclin A2 both in cell cycle regulation and in DNA damage response, identifying small molecule regulators of cyclin A2 activity carries significant potential to regulate diverse cellular processes in both ageing/neurodegeneration and in cancer.

***Objective*:** Based on cyclin A2's recently discovered role in DNA repair, we hypothesized that small molecule inhibitors that were predicted to bind to both cyclin A2 and CDK2 will be useful as a radiosensitizer of cancer cells. In this study, we used structure-based drug discovery to find inhibitors that target both cyclin A2 and CDK2.

***Methods*:** Molecular dynamics simulations were used to generate diverse binding pocket conformations for application of the relaxed complex scheme. We then used structure-based virtual screening to find potential dual cyclin A2 and CDK2 inhibitors. Based on a consensus score of docked poses from Glide and AutoDock Vina, we identified about 40 promising hit compounds, where all PAINS scaffolds were removed from consideration. A biochemical luminescence assay of cyclin A2-CDK2 function was used for experimental verification.

***Results*:** Four lead inhibitors of cyclin A2-CDK2 complex have been identified using a relaxed complex scheme virtual screen have been verified in a biochemical luminescence assay of cyclin A2-CDK2 function. Two of the four lead inhibitors had inhibitory concentrations in the nanomolar range.

***Conclusion*:** The four cyclin A2-CDK2 complex inhibitors are the first reported inhibitors that were specifically designed not to target the cyclin A2-CDK2 protein-protein interface. Overall, our results highlight the potential of combined advanced computational tools and biochemical verification to discover novel binding scaffolds.

Keywords: Cyclin A2, structure-based drug discovery, virtual screening, computational drug discovery, polypharmacology, PAINS.

1. INTRODUCTION

Classical/canonical Cyclin A2 (gene name = CCNA2) activity occurs during S-phase of the cell cycle, where it regulates replication fork initiation and S-G2 progression of cycling cells. Cyclin A2 interacts with cyclin-dependent protein kinase 2 (CDK2) and CDK1 during S-phase and at the G2 -> M transition, respectively [1-4]. However, other non-canonical/non-cell cycle-related cyclin A2 functions have also been documented. For instance, it has been shown that cyclin A2 regulates cytoskeletal architecture [5], plays a role in mRNA translation of the DNA repair gene MRE11 [6], and is required for direct reprogramming of fibroblasts into neurons [7]. Additionally, prior studies demonstrated that Cyclin A2 deletion in neural progenitor cells resulted in cerebellar dysgenesis [8], with phenotypes showing striking similarities to DNA repair mouse mutants. One study showed that reducing Cyclin A2 levels in vitro and in vivo results in a decrease in gH2AX phosphorylation in response to DNA damage [9]. Furthermore, mice with cyclin A2 ablation showed defects in spatial learning and memory as assayed by Barnes Maze, and also showed defects in associative learning as assayed by the Contextual Fear Test [9]. In summary, numerous compelling data demonstrated that cyclin A2 has multiple activities in non-cell cycle activities, the most important of which is its role as a regulator of DNA homeostasis.

Given the diverse roles of cyclin A2 both in cell cycle regulation and in DNA damage response, identifying small molecule regulators of cyclin A2 activity carries the signifi-

*Address correspondence to these authors at the Department of Chemistry and Biochemistry, Ohio State University, Columbus, OH, 43210;
E-mails: lindert.1@osu.edu; jose.otero@osumc.edu
[#]*These authors contributed equally to the work*

1573-4099/21 $65.00+.00

cant potential to regulate diverse cellular processes in both ageing/neurodegeneration and in cancer. Several recent studies link DNA damage to neurodegeneration, including Alzheimer's disease [10]. It has been demonstrated that amyloidogenic transgenic mice, a commonly used experimental model for Alzheimer's disease, show disruptions in DNA repair kinetics that cause abnormal immediate early gene transcription [11]. This abnormal DNA repair kinetics is thought to contribute to cognitive dysfunction in neurodegenerative disorders. Therefore, it has been envisioned that a cyclin A2 agonist could promote DNA repair in neurons and potentially ameliorate neuronal dysfunction in neurodegenerative diseases. In contrast, cyclin A2 loss results in radiosensitization of cancer cells [9]. Radiation treatment induces cancer cell death by promoting DNA double-strand breaks. Chemoradiation therapy is predicated on killing tumor cells while minimizing DNA damage to the surrounding tissues. Hence, it has been envisioned that a cyclin A2-CDK2 complex antagonist could function as a radiosensitizing drug to cancer cells.

Cyclic peptide inhibitors targeting the cyclin binding groove to prevent protein-protein interaction between cyclin A and CDK2 have been reported [12]. Additionally, extensive work has been carried out to achieve inhibition of CDK2 directly. There are 800–900 crystal structures of CDK2 with ligands or inhibitors and most CDK2 inhibitors bind to CDK2 *via* hydrogen bonding interactions (LEU 83, GLU 81), hydrophobic interactions (VAL18, ILE10, ASP146) and Pi-cation interactions (LYS33) [13]. However, none of the deposited structures contain small-molecule ligands that allosterically modulate cyclin A2's activity or target cyclin A2 and CDK2 simultaneously. Additionally, no small allosteric binders have been reported in the literature.

The aim of this study is to simultaneously target cyclin A2 and CDK2 to increase the chance of finding modulators of DNA damage response mechanism. Polypharmacology is a paradigm in drug discovery that searches for multitarget drugs instead of focusing on selective ligands for individual proteins [14]. Studies have shown that many effective drugs act by modulating multiple proteins synergistically, for example, an anticancer drug, lenalidomide, successfully inhibited angiogenesis and metastasis by perturbing multiple proteins' signaling pathway [14-16], and one of the lead compounds of non-bisphophonate farnesyl diphosphate synthase inhibitor also acted as an inhibitor of undecaprenyl diphosphate synthase, which opened up possibilities of multisite targeting for antitumor and anti-infective drug leads [17, 18]. Given cyclin A2's role in DNA repair and its interaction with CDK2, finding small molecule modulators of the cyclin A2-CDK2 complex can be useful in neurodegenerative disease and cancer. The plethora of cyclin A2 structural information can be used for structure-based drug discovery.

Structure-based drug discovery methods are powerful tools in the search for small molecule modulators of proteins [19]. Knowledge of the target protein structure allows for rational virtual high-throughput screening of large libraries of potential small molecule binders. These methods have played a significant role in discovering several FDA-approved drugs [19-21]. Popular molecular docking programs include Glide [22], Fred [23], AutoDock Vina [24], GOLD [25] and FlexX [26]. Recently, methods explicitly accounting for receptor flexibility in computer-aided drug design [27, 28] have shown great promise in structure-based drug discovery. Traditionally, computational docking calculations utilize static receptor structures and allow for the ligand to be flexible. However, methods such as the relaxed complex scheme (RCS) account for both ligand and protein receptor flexibility [1-3], oftentimes by using multiple protein receptor structures extracted from molecular dynamics (MD) simulations starting from a crystal or NMR structure of the receptor of interest. Variations of the RCS have been successfully used in several virtual drug discovery studies [29-45]. Such *in silico* screening methods have been extensively applied to find CDK inhibitors [46, 47] but no similar efforts have also targeted cyclin A2. With the advancement in computational and experimental technology, potential cyclin A2 small molecule binding sites can be identified, probe whether binding site conformations different from those in the crystal structures are more prone to drug binding and finally rationally and efficiently screen for novel modulators that are predicted to target both cyclin A2 and the CDK2 kinase binding site with a higher hit rate than the traditional and more expensive experimental high-throughput library screens.

In this study, structure-based drug discovery is used to find inhibitors that target both cyclin A2 and CDK2. A potential ligand-binding pocket of the cyclin A2 was identified based on crystal structures. MD simulations of cyclin A2 were used to confirm that the pocket is sufficiently accessible by small-molecule binders and to generate diverse binding pocket conformations for application of the relaxed complex scheme. Using a clustering algorithm, five-pocket conformations of the cyclin A2 have been identified that were targeted using virtual screening with Glide and AutoDock Vina. The entire NCI database was screened, and top compound candidates were identified using a consensus scoring approach. Potential PAINS compounds were removed from consideration. About 40 compounds were tested experimentally using a biochemical luminescence assay of cyclin A2-CDK2 function. Two nanomolar range and two micromolar range inhibitors of the cyclin A2-CDK2 complex were verified, and the chemical structures of the potential inhibitors are illustrated in Scheme **1**.

2. METHODS

2.1. Binding Pocket Identification of Cyclin A2

The three-dimensional structure of cyclin A2 has been studied extensively, both in isolation and in complex with its binding partner cyclin-dependent kinase 2 protein (CDK2). Despite the abundant structural information, no structure of cyclin A2 bound to a small molecule ligand exists. It was, thus, necessary to determine possible small molecule binding sites for docking studies. In order to determine the most likely binding location of drug-like molecules to cyclin A2, the cyclin A2 structure (PDB: 4fx3) was submitted to the SITEHOUND binding-site identification server [48]. The SITEHOUND server identified regions of the protein that constitute potential small molecule binding sites by characterizing favorable interactions with a CMET-Methyl Carbon probe. The top 3 binding sites predicted by the

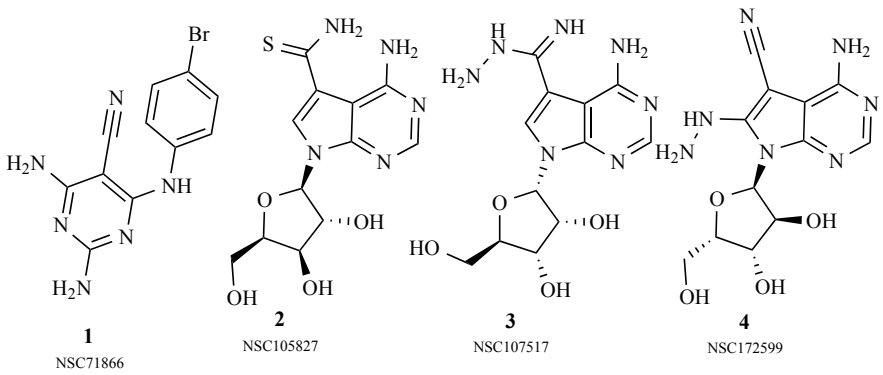

Scheme 1. Identified cyclin A2 inhibitors. The chemical structures of four identified cyclin A2-CDK2 complex inhibitors are shown. Compounds **1** and **2** were identified as potential inhibitors from an initial screening of the NCI diversity set III. Compounds **3** and **4** were identified in a second round of virtual screening of compounds from the NCI database with 80% structural similarity to the seed compound **2**. The chemical structures were generated with ChemDraw.

SITEHOUND were selected, and virtually docked a sample ligand library (NCI Diversity set III [49], consisting of 1,565 small molecule ligands) to each of the 3 potential cyclin A2 binding sites using AutoDock Vina [24]. Based on the ligand efficiencies (AutoDock Vina docking score normalized by number of non-hydrogen ligand atoms) of the docked ligands, site 1 was determined to be the most suitable site for docking studies.

2.2. MD Simulations of Cyclin A2 (System Preparation, NAMD Simulations)

The system prepared for simulations was based on the crystallized structure of the cyclin A2-CDK2 complex (PDB: 4fx3). The cyclin A2 structure (PDB: 4fx3 chain B) was extracted from the crystalized cyclin A2-CDK2 complex. The initial preparation of the system is described in the study [38]. In short, the system was solvated in a TIP3P water box and Na^+ and Cl^- ions were added to neutralize the system and set up an ionic strength of 0.15 M. The fully solvated cyclin A2 system contained 48,110 atoms. The system was minimized and equilibrated prior to running a 100 ns MD simulation. MD simulations were performed using the CHARMM22 [50] force field. Particle Mesh Ewald (PME) and periodic boundary conditions were applied to the system with a nonbonded interaction cutoff of 12 Å. Bonds involving hydrogen atoms were constrained using the SHAKE algorithm. Cyclin A2 was simulated for 100 ns with a time step of 2 fs, resulting in a total of 50,000 frames.

2.3. Pocket Volume and Shape Analysis of Cyclin A2

To quantify the volume and dimensions of the potential cyclin A2 binding pocket, POVME was used for volume measurement [51]. The following coordinates, which encompassed the potential binding site region, were used as sphere centers for a POVME inclusion sphere: (18.5, 5.0, 12.7). Points were generated in POVME with a grid spacing of 1 Å using an inclusion sphere radius of 7.5 Å around the above sphere centers. The distance cutoff was set at 1.09 Å, thus any point that came within this distance from the receptor atom was not considered for the pocket volume calculation.

2.4. Clustering Analysis of the Cyclin A2 MD Trajectory

Structures representing the conformational variability of the binding site during the simulation were extracted using clustering. For clustering, every fourth frame was extracted from the MD trajectory. A sample ligand was docked to the binding site with AutoDock Vina and the docked pose was used as the ligand-bound reference structure for clustering. The alignment was based on all C-alpha atoms within 10 Å of the ligand in the ligand-bound reference structure. Clustering was performed by RMSD using GROMOS++ conformational clustering tool [52]. An RMSD cutoff of 0.9 Å was chosen, resulting in five clusters that represented at least 90% of the trajectory. The central members of each of these clusters were chosen to represent the protein conformations within the cluster and thereby the pocket conformations sampled by the trajectory.

2.5. Screening Library Preparation

The NCI Diversity set III, a diverse and representative subset of the entire NCI database containing 1,565 unique compounds, was used for the virtual screening. Prior to any virtual screening, all PAINS compounds [53] were removed from the screening library. PAINS compounds are chemical compounds that nonspecifically interact with biological targets and consequently tend to generate false-positive results in high-throughput screens. Therefore, filtering PAINS compounds from the ligand database reduced the chance of obtaining false positive hits in our biochemical assay. PAINS compounds were filtered using the PAINS-Remover server [54]. The compounds were submitted to the server in SMILES format. After the PAINS filtration of the NCI Diversity set III, the ligand library consisted of 1,473 compounds. Prior to virtual screening, compounds were prepared using Schrödinger's LigPrep package [55]. Tautomers and possible chiralities of each compound were generated. The energy minimization step was conducted using the OPLS_2005 force field, and compounds were ionized at a target pH of 7.0 ± 2.0.

2.6. Initial Virtual Screening with Glide Against CDK2 and Cyclin A2

In order to identify modulators that are predicted to target both cyclin A2 and the CDK2 kinase binding site, the NCI Diversity set III compounds were screened into two binding sites: the newly identified binding pocket of cyclin A2 (PDB: 4fx3 chain B) and CDK2 kinase site (PDB: 4fx3

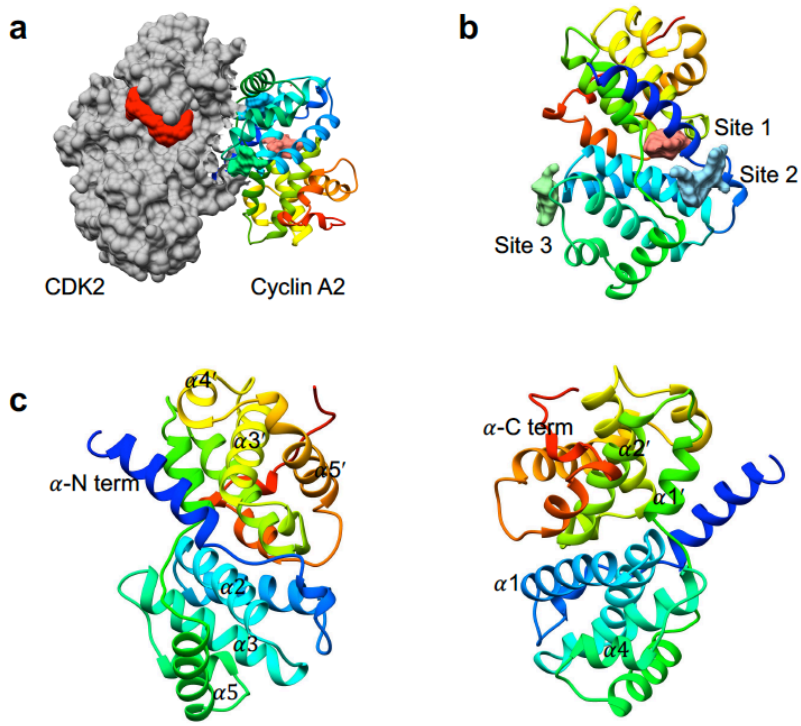

Fig. (1). Cyclin A2-CDK2 complex and Cyclin A2 with top 3 potential binding sites. (a) Cyclin A2 is shown in rainbow colors and CDK2 is shown in grey, illustrating the binding surface of cyclin A2 involved in protein-protein interaction with CDK2. The ATP binding site of CDK2 is colored in red. **(b)** The top 3 binding sites predicted by the SITEHOUND server are colored in pink, light-blue, and green for site 1, site 2, and site 3, respectively. Sites 2 and 3 were located on the surface of cyclin A2, whereas site 1 was more embedded within the protein. **(c)** Two different views of cyclin A2, with all alpha-helices being labeled. *(A higher resolution / colour version of this figure is available in the electronic copy of the article).*

chain A), as shown in Fig. (**1**). The NCI Diversity set III was docked to five previously identified representative cyclin A2 binding pocket conformations and a crystalized structure of CDK2 (4fx3 chain A) using both AutoDock Vina and Glide. The docking site of cyclin A2 was centered at x = 18, y = 3, and z = 10 coordinates, whereas the CDK2 was centered at x = -10, y =8, and z = 35. For Autodock Vina, the target's box size was set to be 25Åx25Åx25Å. For Schrödinger's Glide, the grid was centered at the target's docking site coordinates with an inner box size of 20Åx20Åx20Å, and an outer box size of 40Åx40Åx40Å. In Glide, the selected compounds were docked to the cyclin A2 binding site with the OPLS_2005 forcefield, the van der Waals radii of ligand atoms were scaled by 0.8, a charge cutoff for polarity was set at 0.15, and the GlideScore version XP5.0 was used.

For each target, compounds were first ranked based on their Autodock Vina affinity score and the Glide XP docking score, then the consensus rank of the two docking tools (defined as the sum of Glide and Vina rank) was applied. Since the aim of this study was to identify small molecules that could interact with both the cyclin A2 and the CDK2 binding sites, the two consensus ranked compound list, and ranked the compounds by the consensus rank of the two targets were merged (defined as the sum of cyclin A2 and CDK2 rank). Different weights were applied to the two targets when calculating the consensus rank, in order to obtain more compounds that are likely to interact with cyclinA2. 70% of the cyclin A2 rank and 30% of the CDK2 rank for the consensus rank of the two targets were used. The top 20 compounds were selected based on their final consensus rank and visual inspection. An initial screening *in vitro* biochemical assay (see below) was utilized to verify the functional activity of the selected 20 compounds and confirmed two compounds (compound **1** or NSC71866, and compound **2** or NSC105827) as inhibitors of the cyclin A2-CDK2 complex.

2.7. Ligand Similarity Search

The dataset used to identify the two initial hit compounds, the NCI Diversity set III, covered less than 1% of all NCI database compounds (250,250 chemical molecules). For the purpose of hit improvement, compounds from the entire NCI database were identified, which were structurally similar to the two hit compounds (compounds **1** and **2**) with verified *in vitro* biochemical activity. The similarity search function of the database was utilized and a similarity cutoff of 80% Tanimoto similarity was used. The derived compound set contained 471 compounds (157 compounds similar to compound **1**; 314 compounds similar to compound **2**). Prior to virtual screening, any PAINS compounds were again removed from the ligand set. As a result, 463 compounds remained after PAINS filtration (151 compounds similar to compound **1**; 312 compounds similar to compound **2**). Once again, in order to identify modulators that would target both cyclin A2 and CDK2 binding sites, the filtered 463 compounds were screened against the cyclin A2 and the CDK2 kinase binding site using AutoDock Vina and GlideXP 5.0. Compounds were docked to the previously identified five representative cyclin A2 binding pocket conformations and a

crystalized structure of CDK2. Again, the top 20 compounds from this screening were selected based on the weighted consensus rank of the two targets and visual inspection. A second round of *in vitro* biochemical verification was utilized to assess the functional activity of these additional 20 compounds.

2.8. Experimental Verification Assay

The ADP-Glo™ Kinase Assay was carried out in 96-well plates. The kinase detection buffer and Kinase detection reagent were previously prepared according to the manufacturer's recommendations. Each experimental compound was diluted in DMSO to a concentration of 1mM. The reaction buffer was prepared by adding 200μM DTT to 4x diluted 5X Reaction Buffer A (200mM Tris [pH 7.5], 100mM MgCl2 and 0.5mg/ml BSA). Compounds were diluted into 10μM and 1μM in the reaction buffer, briefly centrifuged at 840 rpm, and incubated for 60 minutes with Cyclin A2-CDK2 kinase enzyme and 5ul of ATP/Substrate mix. The ATP/Substrate was prepared by adding Histone H1 (1mg/ml) to 150μl of 500μM of ATP into reaction buffer. Then, 5 μl of ADP-Glo™ reagent was incubated for 40 minutes to stop kinase reaction after being centrifuged at 840 rpm. The kinase detection reagent was added in the ratio 2:1:1 of kinase reaction and ADP-Glo™ reagent to convert ADP to ATP in 30 minutes. The luminescence was measured in a Synergy™ H1 Biotek plate reader. The Reaction Biology Corporation was contracted to determine dose-response curves of four compounds (Compound **1**, **2**, **3**, and **4**), and the following final concentrations: 0nM, 5nM, 15nM, 45nM, 0.1μM, 0.4μM, 1.2μM, 3.7μM, 11μM, 33μM, and 100μM of each compound were used. All steps were performed at room temperature (22-25°C). Staurosporine was used as an inhibitor of Cyclin A2-CDK2 kinase action and thus as a positive control for enzyme inhibition. DMSO with enzyme was used as the control reaction, and DMSO without enzyme was used as the "blank" for the luminometer.

2.9. Predicting Binding Targets *via* Cross-docking

In order to predict the binding target of the inhibitors, the TargetID python script was used [56]. Compounds for target screening were prepared using Schrödinger's LigPrep package prior to virtual screening. The energy minimization step was conducted using the OPLS_2005 force field, and compounds were ionized at a target pH of 7.0 +- 2.0. All the selected compounds were docked to cyclin A2 and CDK2 binding sites using GlideScore version SP 5.0. For cyclin A2, the grid was centered at x = 18, y = 3, and z = 10 coordinates, with an inner box size of 20Åx20Åx20Å, and an outer box size of 45Åx45Åx45Å. For CDK2, the grid was centered at x = -10, y = 8, and z = 35 coordinates, with an inner box size of 20Åx20Åx20Å, and an outer box size of 40Åx40Åx40Å.

3. RESULTS AND DISCUSSION

Based on cyclin A2's recently discovered role in DNA repair, it has been hypothesized that small molecule inhibitors that were predicted to bind to both cyclin A2 and CDK2 will be useful as a radiosensitizer of cancer cells. Here it has been observed that cyclin A2 structural information can be used for structure-based drug discovery. Cyclin A2 is a challenging receptor target for structure-based drug discovery, since no small molecules of cyclin A2 have been reported and no ligand-bound structures of cyclin A2 or any other cyclin family members have been determined. Thus, potential binding sites are unknown. A potential ligand-binding pocket based on structural information from crystal structures has been identified. MD simulations were used to confirm that the pocket is sufficiently accessible by small-molecule binders and to generate diverse binding pocket conformations to account for receptor flexibility. Since protein flexibility plays a central role in biomolecular recognition, incorporating dynamic receptor conformations in virtual ligand docking has been demonstrated to be helpful [27]. Five distinct pocket conformations were targeted using virtual screening with Glide and AutoDock Vina. The NCI database was screened against both the identified cyclin A2 binding sites and the CDK2 kinase binding site, and top compound candidates were identified using a consensus scoring approach. Potential PAINS compounds were removed from consideration. About 40 compounds were tested experimentally using a biochemical luminescence assay. Two nanomolar and two micromolar inhibitors that are predicted to target both cyclin A2 and CDK2, were verified.

3.1. Pocket Identification of Cyclin A2 and Verification

The SITEHOUND server was used to identify potential cyclin A2 binding sites. The top 3 ranked potential binding sites were selected for further verification. The locations of the top 3 predicted cyclin A2 binding sites were distinct and the binding site volume varied for each site. According to the SITEHOUND server, the volume of site 1 was 86 $Å^3$, 74 $Å^3$ for site 2, and 53 $Å^3$ for site 3. As shown in Fig. (**1**), site 1 was embedded inside the cyclin A2 protein, delineated by the central parts of helices α1, α2, α2′ and α3′. Site 2 was located on the surface of cyclin A2, between α-N terminal and α5. Site 3 was located near the cyclin binding groove, on the surface between α1 and the loop that links α3 and α4. In order to select the most favorable of the binding sites identified by SITEHOUND for interactions with drug-like molecules, a sample ligand library (NCI Diversity set III) to each of the three potential cyclin A2 binding sites using AutoDock Vina was virtually docked. A total of 1,565 unique ligands were docked to each of the three potential binding sites of cyclin A2. The ligand efficiencies (AutoDock Vina docking score normalized by number of heavy ligand atoms) of the docked ligands to determine the most suitable of the three sites for docking studies were used. As a result, the average of the top 100 ligand efficiencies was -0.5675 for site 1. This was higher than the average ligand efficiencies for the other two sites (site 2: -0.5672; site 3: -0.4202). In addition, site 1 was the only site out of the three that did not directly interfere with the protein-protein interface. Site 1 was thus chosen for all following docking studies. Site 1 comprised 36 hydrophobic residues (56.25%), 16 polar neutral residues (25%), and 12 charged residues (18.75%) (5 acidic residues and 7 basic residues).

3.2. MD Simulation: Ligand Accessibility

Even though the virtual docking supported site 1 as the binding pocket to have the most favorable interaction with

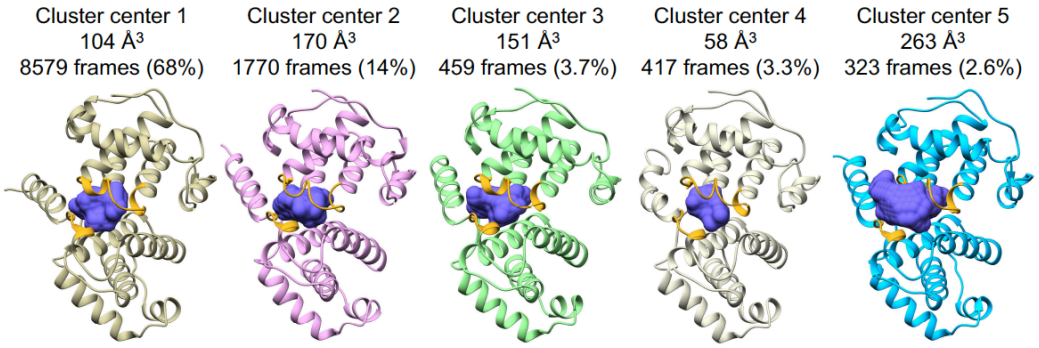

Fig. (2). Pocket volume analysis of five key binding conformations of cyclin A2. Five cluster centers from an MD simulation, identified as representative conformations of the potential cyclin A2 binding site, are shown. Each binding conformation is depicted in a different color, and the binding pockets are colored in purple surface representation. The residues that are involved in the opening of cyclin A2 are colored in yellow. Additionally, the volume of the binding pockets and the size of the respective cluster (in number of frames and percentage) are provided. *(A higher resolution / colour version of this figure is available in the electronic copy of the article).*

drug-like molecules, the buried nature of site 1 had the potential to reduce potential external interactions. Therefore, a 100 ns molecular dynamics simulation was utilized to investigate whether the embedded binding pocket opened up frequently and became sufficiently exposed to the surrounding environment, thereby increasing the accessibility of potential drug-like molecules. From the 100 ns trajectory, the loop that connected α-N terminal and α1 was flexible (from LYS194 to LYS201). This loop moved away from the loop that connected α2′ and α3′ (from SER340 to PRO352), consequently exposing the embedded site 1 to the external environment. This large opening of site 1 was short-lived (3% of the trajectory), but sufficient for small, drug-like molecules to enter and interact with this potential cyclin A2 binding site.

After having confirmed the suitability of site 1 for structure-based drug discovery, a clustering analysis was used to extract structures representing the conformational variability of the cyclin A2 binding site during the simulation. For the clustering analysis, every fourth frame of the 100 ns MD trajectory was extracted and similar binding site conformations were grouped as clusters. As a result, five cluster centers were identified as representative conformations of the potential cyclin A2 binding site (Fig. **2**). As illustrated in Fig. **2**, site 1 exhibited a pocket volume size ranging from 104 $Å^3$ to 170 $Å^3$ for about 85% of the trajectory (cluster1, cluster2, and cluster3). Cluster 5, which represented about 3% of the trajectory, corresponded to a completely open conformation of cyclin A2.

3.3. Virtual Screening of NCI Diversity set III with Glide and AutoDock Vina

Using both AutoDock Vina and Glide, 1,473 NCI Diversity set III compounds (PAINS compounds had been removed from the screening dataset) were docked into each of the five cyclin A2 cluster centers and to CDK2. For each target, compounds were then individually ranked according to their Autodock Vina affinity score and their Glide XP docking score. In order to optimize the selection of potential hits, the docked compounds were subsequently sorted by their consensus rank, *i.e.* the sum of their individual Glide and Vina ranks. The two lists of consensus rank were then merged (cyclin A2 and CDK2) by a weighted consensus rank of the two targets. This consensus ranking approach ensured the selection of compounds that performed well in both scoring functions and both cyclin A2 and CDK2. There is empirical evidence that the use of multiple force fields improves sampling and prediction accuracy in the areas of molecular dynamics, protein structure prediction, protein-ligand docking and protein-protein docking. In structure-based protein-ligand docking particularly, consensus scoring has been reported to substantially improve virtual screening performance, contributing to better enrichments, while also improving the prediction of bound conformations and poses [57-60]. As shown in Table **S1**, the top 20 compounds' Vina affinity scores of cyclin A2 and CDK2 ranged from -6.5 to -9.7 kcal/mol, and Glide XP docking scores of cyclin A2 and CDK2 ranged from -5.5 to -9.6 kcal/mol. Among the five cluster centers, the preferred cyclin A2 conformations targeted by the top 20 compounds were cluster center 2 (volume: 170 $Å^3$) and cluster center 3 (volume: 151 $Å^3$). As shown in Table **S1**, 15 out of top 20 compounds favored docking into cluster center 2 for Vina. For Glide, 11 compounds favored cluster center 2 while 9 compounds favored cluster center 3. Thus, based on the virtual docking results, the favorable cyclin A2 binding conformations were the ones with binding pocket volume sizes ranging between 150 $Å^3$ to 170 $Å^3$. This was encouraging since those two cluster centers also accounted for more than 85% of the MD simulation trajectory and thus, they likely constitute predominant cyclin A2 pocket conformations *in vitro*.

3.4. Experimental Screening of top 20 Compounds from NCI Diversity Set III

The top 20 compounds identified in the combined AutoDock Vina and Glide virtual screen were ordered from the National Cancer Institute Development Therapeutic Program. In order to verify the functional activity of the selected top 20 compounds, various compound concentrations (0μM 1μM, and 10μM) were applied in an *in vitro* biochemical assay that quantified the kinase activity of the cyclin A2-CDK2 complex. As shown in Fig. (**3**), two inhibitors (compound **1** and **2**) were identified. Between the two potential inhibitors, compound **2** was the more effective inhibitor compared to compound **1**, since 1μM of compound **2** re-

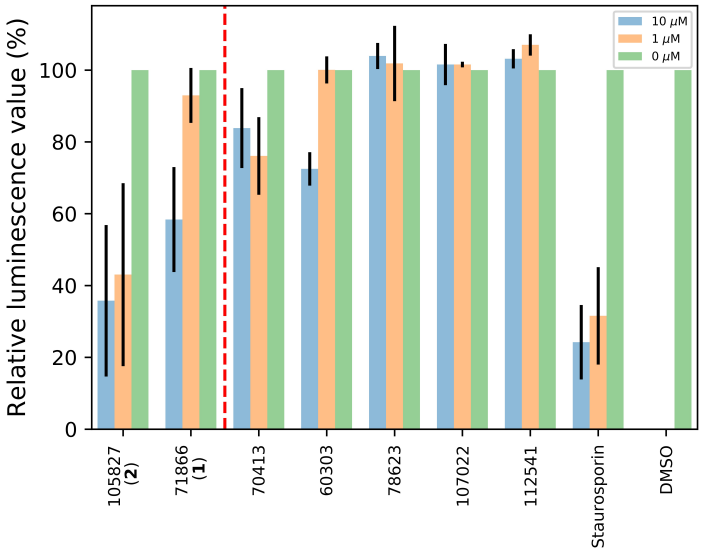

Fig. (3). ***In vitro*** **Screening of the top 20 compounds from NCI diversity set III.** Selected top 20 compounds were screened using a kinase assay. Results for seven compounds are shown. The bar graph is showing the relative luminance of two identified inhibitors (compounds **1** and **2**), and five randomly selected compounds, which showed little to no inhibition, a known kinase inhibitor (Staurosporine), and a negative control (DMSO). Each compound was tested at various concentrations (0μM, 1μM, and 10μM). The red dash line separates the two identified inhibitors from the five top ranked compounds. Error bars are showing the standard error of the mean (SEM). *(A higher resolution / colour version of this figure is available in the electronic copy of the article).*

duced CDK2 kinase activity to 43%, whereas compound **1** had no significant effect at a concentration of 1 μM. Increasing the concentration of compound **2** to 10 μM did not further reduce the kinase activity. Compound **1**, on the other hand, reduced the kinase activity to 58% at the highest concentration (10μM of compound **1**). Encouragingly, compound **2** inhibited CDK2 kinase activity at levels similar to the known CDK2 inhibitor Staurosporin. The kinase activity of all 20 compounds is illustrated in Supplemental Fig. (**1**).

The docked poses of compounds **1** and **2** in cyclin A2 binding site were investigated. According to the binding conformations generated using AutoDock Vina and Glide, compound **1** favored cluster center 3, while compound **2** preferred cluster center 2. As shown in Supplemental Fig. (**2**), compound **1** formed four favorable hydrogen bonds with residues in the binding site (SER340, ASP343, TYR347, and TYR199), and compound **2** formed six favorable hydrogen bonds with the binding site residues (SER340, TYR347, ALA344, PRO309, and HSD233). Across both potential inhibitors, the common interacting residues were SER340 and TYR347.

3.5. Second Round of Virtual screening of Compounds Similar to Initial Hits

From the initial virtual screening of 1,473 NCI Diversity set III compounds, the top 20 hits were selected for *in vitro* verification, and successfully identified two potential cyclin A2-CDK2 complex inhibitors among those 20 compounds. To capitalize on the success of the potential inhibitors from the initial screen, the ligand library for virtual screening was expanded to the entire NCI database. For an efficient search of potential additional modulators, the focus is on compounds with high structural similarity (≥ 80% Tanimoto similarity) to the two initial hits (compounds **1** and **2**). It has been hypothesized that compounds that are structurally similar to the potential ligands will exhibit comparable and potentially increased functional activity in follow-up *in vitro* screening. A similarity search yielded 471 compounds which were subsequently filtered to remove known Pan-Assay Interference Compounds (PAINS). As a result, filtered compounds were docked into each of the five cyclin A2 cluster centers and to the CDK2 binding site using both AutoDock Vina and Glide. Again, the compounds docked into each of the targets were individually ranked according to their Autodock Vina affinity score and their Glide XP docking score, respectively, followed by a weighted consensus rank sorting. As shown in Table **S2**, the top 20 consensus compounds' Vina affinity score of cyclin A2 and CDK2 ranged from -6.7 to -9.8 kcal/mol, and Glide XP docking scores of cyclin A2 and CDK2 ranged from -4.2 to -11.9 kcal/mol. Among the five cluster centers, the most favored cyclin A2 conformations were again cluster centers 2 and 3, as shown in Table **S2**.

3.6. Experimental Result: Similarity 80% Ligands

To test the extent to which these compounds inhibited cyclin A2-CDK2 activity, the ADP-Glo^{TM} Kinase Assay, an assay that tests the capacity of cyclin A2-CDK2 complexes to phosphorylate targets was utilized. As a positive control for reaction inhibition, a staurosporine treatment condition that abrogates all kinase activity in the reaction was included. As a negative control, the vehicle (i.e., DMSO) was used, in addition to a DMSO without cyclin A2 to serve as a blank reading for the luminometer. The top 20 compounds identified in the second virtual screen of similar compounds were ordered from the NCI Development Therapeutic Program. *In vitro* follow-up experiments tested various compound concentrations (0μM, 1μM and 10μM) and quantified their effect on the kinase activity of the cyclin A2-CDK2 complex.

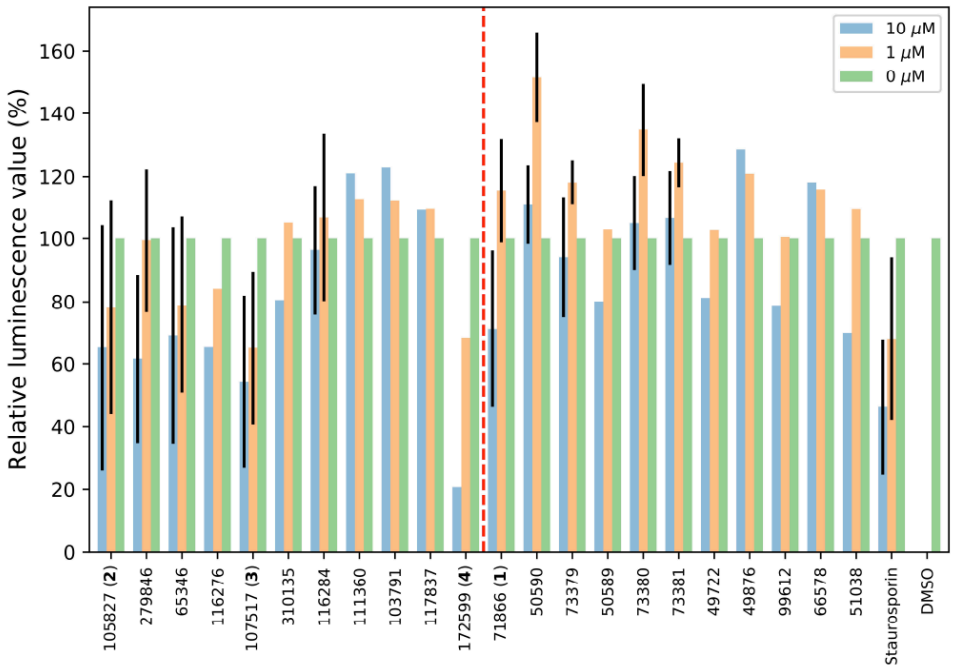

Fig. (4). ***In vitro*** **Screening of the top 20 compounds of structural similarity to initial hits.** The selected top 20 compounds were screened with the kinase assay. For each seed ligand (compounds **1** and **2**), ten structurally similar compounds were selected for *in vitro* screening. The relative luminescence value of compounds with 80% structural similarity to the two inhibitors (compounds **1** and **2**), a known kinase inhibitor (Staurosporine) and negative control (DMSO) are shown. Each compound was tested at various concentrations (0μM, 1μM, and 10μM). Compounds on the left side of the red dash line were derived from compound **2**, and compounds on the right were derived from compound **1**. Error bars are showing the standard error of the mean (SEM). *(A higher resolution / colour version of this figure is available in the electronic copy of the article).*

As expected, the majority of the tested compounds showed similar functional activity as their seed ligands (compound **1** and **2**). As illustrated in Fig. (**4**), five of the compounds with 80% structural similarity to compound **2** (NSC279846, NSC65346, NSC116276, NSC107517, and NSC172599) exhibited a similar trend of inhibition as their seed compound **2**. Among these five compounds, compounds **3** and **4** approximately inhibited CDK2 activity as effectively as Staurosporin at 1μM, inhibiting the kinase activity to 65% and 68%, respectively. Encouragingly, compound **4** inhibited CDK2 kinase activity to 20% at 10 μM, which was stronger than the known CDK2 inhibitor Staurosporin (46%). Compounds with 80% structural similarity to compound **1**, on the other hand, showed little to no inhibition. Interestingly, five of those compounds (NSC50590, NSC73380, NSC73381, NSC49876, and NSC66578) even weakly activated CDK2 activity at 10μM, as shown in Fig. (**4**).

3.7. Dose-Response

From the second set of 20 compounds, the four most promising inhibitors (compounds **1**, **2**, **3** and **4**) were selected and tested for dose-response. For the purpose of dose-response measurements, various concentrations of the selected four compounds (0nM, 5nM, 15nM, 45nM, 0.1μM, 0.4μM, 1.2μM, 3.7μM, 11μM, 33μM, and 100μM) were applied in the *in vitro* biochemical assay that quantified the kinase activity of the cyclin A2-CDK2 complex. The selected compounds' dose-response was compared with the known kinase inhibitor, Staurosporine. As shown in Fig. (**5**), the IC50 values of the four compounds were 6.5 μM, 7.6 nM, 181 nM, and 1.9 μM for compounds **1** through **4**, respectively. Two inhibitors (compounds **2** and **3**) showed IC50 values in the nanomolar range, where compound **2** was the most effective inhibitor among the four compounds with a low nanomolar IC50. Notably, compound **2**'s cyclin A2-CDK2 inhibition was as potent as the known kinase inhibitor Staurosporine (IC50 1nM).

The docked poses of compounds **3** and **4** in cyclin A2 binding site were also investigated**.** According to the binding conformations generated using AutoDock Vina and Glide, compound **3** and **4** favored cluster center 3 of the cyclin A2 for Glide. As shown in Supplemental Fig. (**3**), compound **3** formed eight favorable hydrogen bonds with residues in the binding site (SER340, ASP343, ALA344, TYR350, ASN237, and PRO309) and compound **4** formed seven favorable hydrogen bonds with binding site residues (SER340, TYR350, TYR347, PRO309, ASP240, and ARG211). Indeed, both backbone and side chain atoms of SER340 were predicted to form hydrogen bonds with compound **4**. Interestingly, SER340 was the most common residue interacting with all of the potential inhibitors (compounds **1**, **2**, **3**, and **4**). PRO309 was the most common residue for the seed compound **2** and its structurally similar compounds (compound **3** and **4**), whereas TYR350 residue was only found in compounds **3** and **4**.

In addition to virtual screening, and selecting compounds based on their weighted consensus ranking, the TargetID target identification application [56] was used to predict binding target of the identified inhibitors. According to the TargetID application, compounds **1** and **3** were predicted to

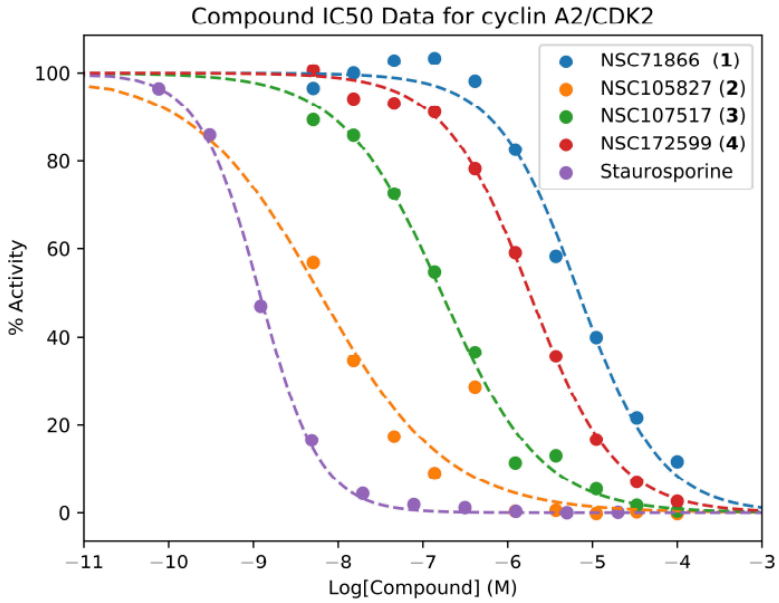

Fig. (5). ***In vitro*** **dose response of compound 1, 2, 3, and 4.** The kinase activity of the selected four compounds was tested at various concentrations (0nM, 5nM, 15nM, 45nM, 0.1µM, 0.4µM, 1.2µM, 3.7µM, 11µM, 33µM, and 100µM). The relative kinase activity values of the potential inhibitors (compounds **1**, **2**, **3**, and **4**) and the known CDK inhibitor Staurosporine at various concentrations are shown. IC50 values of the four compounds were 6.5µM (**1**), 7.6nM (**2**), 181nM (**3**), and 1.9µM (**4**), respectively. The IC50 of the known CDK inhibitor Staurosporine was 1nM. *(A higher resolution / colour version of this figure is available in the electronic copy of the article).*

bind to the cyclin A2 binding site over the CDK2 kinase binding site, whereas the remaining two compounds (compounds **2** and **4**) were predicted to bind to the CDK2 kinase binding site. The combined Z-scores, as determined by TargetID, of the four inhibitors were -0.39 (compound **1**), -0.66 (compound **2**), -1.48 (compound **3**), and -0.90 (compound **4**), respectively. Interestingly, compounds that were predicted to preferentially interact with the cyclin A2 binding site (compounds **1** and **3**) generally exhibited micromolar range IC50 values, whereas the remaining compounds (compounds **2** and **4**) exhibited nanomolar range IC50 values.

CONCLUSION

Recent studies have shed light on cyclin A2's critical role in DNA repair, making it an attractive target for neurodegenerative disease and cancer drug discovery. Here, a novel potential cyclin A2 allosteric ligand-binding pocket was identified, and a combination of molecular dynamics and virtual screening structure-based drug discovery to find candidate cyclin A2-CDK2 complex inhibitors was used. A number of leads for cyclin A2-CDK2 complex inhibitors have been identified using a relaxed complex scheme virtual screen of this allosteric site and the CDK2 binding site and have been verified in a biochemical luminescence assay of cyclin A2-CDK2 function. The most potent leads, compounds **2** and **3** were all ribofuranosyl-pyrrolo[2,3-d]pyrimidines with inhibitory concentrations in the nanomolar range. Three of the selected compounds (compounds **2**, **3**, and **4**) do appear to have a structural resemblance of ATP, however, as determined by the Tanimoto similarity index employing RDKit's Daylight fingerprinting method, the three compounds are only about 60% structurally similar with ATP. According to research at Abbott Laboratories, structures will be considered highly homologous if their Tanimoto index/Daylight fingerprint exceeds 0.85 [61]. Similarly, compound **1** has only 51% structural similarity with known CDK2 inhibitor PNU 112455A (PDB: 1JSV). Furthermore, the TargetID target identification application [56] was used to predict the receptors of each of the compounds. Compounds **1** and **3** were predicted to bind to the cyclin A2 binding site over the CDK2 kinase binding site suggesting that they likely inhibit the kinase activity through cyclin A2 inhibition. Importantly, the docking scores of compounds **1**, **2**, **3**, and **4** ranged from -5.5 to -6.2 kcal/mol when docked into the cyclin A2 crystal structure. Consequently, they would have never been picked for experimental verification, underscoring the importance of our use of the relaxed complex scheme to account for receptor flexibility. Compounds **1**, **2**, **3**, and **4** were only identified using structures from a molecular dynamics simulation. Interestingly, we observed several weak activators in our screens and we will focus future work to pursue potential cyclin A2 activation which has implications in neurodegenerative disease. Future work will focus on identification of additional non-nucleoside inhibitors. Additionally, future studies will concentrate on experimental verification of the binding targets of our potential hit compounds. Overall, our results highlight the potential of combined advanced computational tools and biochemical verification to discover novel binding scaffolds.

ETHICS APPROVAL AND CONSENT TO PARTICIPATE

Not applicable.

HUMAN AND ANIMAL RIGHTS

No animals/humans were used for studies that are the basis of this research.

CONSENT FOR PUBLICATION

Not applicable.

AVAILABILITY OF DATA AND MATERIALS

The data that support the findings of this study are available from the corresponding author upon reasonable request.

FUNDING

The authors would like to thank the members of the Lindert lab for many useful discussions, Behiye Kaya for helping with some assays, and the Reaction Biology Corporation for providing dose response curve data of the compounds. We would like to extend a special thanks to Mark Foster for his efforts to express cyclin A2. We would like to thank the Ohio Supercomputer Center for valuable computational resources [62]. This work was supported by NIH (R03 AG054904; https://doi.org/10.13039/100000049) to S.L. Additionally, work in the Lindert laboratory is supported through NIH (R01 HL137015), NSF (CHE 1750666) and a Falk Medical Research Trust Catalyst Award. Work in the Otero lab is supported by R01HL132355.

CONFLICT OF INTEREST

The authors declare no conflict of interest, financial or otherwise.

ACKNOWLEDGEMENTS

Declared none.

SUPPLEMENTARY MATERIAL

Supplementary material is available on the publisher's website along with the published article.

REFERENCES

[1] Amaro, R.E.; Baron, R.; McCammon, J.A. An improved relaxed complex scheme for receptor flexibility in computer-aided drug design. **J. Comput. Aided Mol. Des.**, **2008**, **22**(9), 693-705. http://dx.doi.org/10.1007/s10822-007-9159-2 PMID: 18196463

[2] Lin, J.H.; Perryman, A.L.; Schames, J.R.; McCammon, J.A. The relaxed complex method: Accommodating receptor flexibility for drug design with an improved scoring scheme. **Biopolymers**, **2003**, **68**(1), 47-62. http://dx.doi.org/10.1002/bip.10218 PMID: 12579579

[3] Lin, J-H.; Perryman, A.L.; Schames, J.R.; McCammon, J.A. Computational drug design accommodating receptor flexibility: the relaxed complex scheme. **J. Am. Chem. Soc.**, **2002**, **124**(20), 5632-5633. http://dx.doi.org/10.1021/ja0260162 PMID: 12010024

[4] Pagano, M.; Pepperkok, R.; Verde, F.; Ansorge, W.; Draetta, G. Cyclin A is required at two points in the human cell cycle. **EMBO J.**, **1992**, **11**(3), 961-971. http://dx.doi.org/10.1002/j.1460-2075.1992.tb05135.x PMID: 1312467

[5] Arsic, N.; Bendris, N.; Peter, M.; Begon-Pescia, C.; Rebouissou, C.; Gadéa, G.; Bouquier, N.; Bibeau, F.; Lemmers, B.; Blanchard, J.M. A novel function for Cyclin A2: control of cell invasion via RhoA signaling. **J. Cell Biol.**, **2012**, **196**(1), 147-162. http://dx.doi.org/10.1083/jcb.201102085 PMID: 22232705

[6] Kanakkanthara, A.; Jeganathan, K.B.; Limzerwala, J.F.; Baker, D.J.; Hamada, M.; Nam, H.J.; van Deursen, W.H.; Hamada, N.; Naylor, R.M.; Becker, N.A.; Davies, B.A.; van Ree, J.H.; Mer, G.; Shapiro, V.S.; Maher, L.J., III; Katzmann, D.J.; van Deursen, J.M. Cyclin A2 is an RNA binding protein that controls Mre11 mRNA translation. **Science**, **2016**, **353**(6307), 1549-1552. http://dx.doi.org/10.1126/science.aaf7463 PMID: 27708105

[7] Gallego-Perez, D.; Otero, J.J.; Czeisler, C.; Ma, J.; Ortiz, C.; Gygli, P.; Catacutan, F.P.; Gokozan, H.N.; Cowgill, A.; Sherwood, T.; Ghatak, S.; Malkoc, V.; Zhao, X.; Liao, W.C.; Gnyawali, S.; Wang, X.; Adler, A.F.; Leong, K.; Wulff, B.; Wilgus, T.A.; Askwith, C.; Khanna, S.; Rink, C.; Sen, C.K.; Lee, L.J. Deterministic transfection drives efficient nonviral reprogramming and uncovers reprogramming barriers. **Nanomedicine (Lond.)**, **2015**. PMID: 26711960

[8] Otero, J.J.; Kalaszczynska, I.; Michowski, W.; Wong, M.; Gygli, P.E.; Gokozan, H.N.; Griveau, A.; Odajima, J.; Czeisler, C.; Catacutan, F.P.; Murnen, A.; Schüller, U.; Sicinski, P.; Rowitch, D. Cerebellar cortical lamination and foliation require cyclin A2. **Dev. Biol.**, **2014**, **385**(2), 328-339. http://dx.doi.org/10.1016/j.ydbio.2013.10.019 PMID: 24184637

[9] Gygli, P.E.; Chang, J.C.; Gokozan, H.N.; Catacutan, F.P.; Schmidt, T.A.; Kaya, B.; Goksel, M.; Baig, F.S.; Chen, S.; Griveau, A.; Michowski, W.; Wong, M.; Palanichamy, K.; Sicinski, P.; Nelson, R.J.; Czeisler, C.; Otero, J.J. Cyclin A2 promotes DNA repair in the brain during both development and aging. **Aging (Albany NY)**, **2016**, **8**(7), 1540-1570. http://dx.doi.org/10.18632/aging.100990 PMID: 27425845

[10] Madabhushi, R.; Pan, L.; Tsai, L.H. DNA damage and its links to neurodegeneration. **Neuron**, **2014**, **83**(2), 266-282. http://dx.doi.org/10.1016/j.neuron.2014.06.034 PMID: 25033177

[11] Suberbielle, E.; Sanchez, P.E.; Kravitz, A.V.; Wang, X.; Ho, K.; Eilertson, K.; Devidze, N.; Kreitzer, A.C.; Mucke, L. Physiologic brain activity causes DNA double-strand breaks in neurons, with exacerbation by amyloid-β. **Nat. Neurosci.**, **2013**, **16**(5), 613-621. http://dx.doi.org/10.1038/nn.3356 PMID: 23525040

[12] Brown, N.R.; Noble, M.E.; Endicott, J.A.; Garman, E.F.; Wakatsuki, S.; Mitchell, E.; Rasmussen, B.; Hunt, T.; Johnson, L.N. The crystal structure of cyclin A. **Structure**, **1995**, **3**(11), 1235-1247. http://dx.doi.org/10.1016/S0969-2126(01)00259-3 PMID: 8591034

[13] Andrews, M.J.; McInnes, C.; Kontopidis, G.; Innes, L.; Cowan, A.; Plater, A.; Fischer, P.M. Design, synthesis, biological activity and structural analysis of cyclic peptide inhibitors targeting the substrate recruitment site of cyclin-dependent kinase complexes. **Org. Biomol. Chem.**, **2004**, **2**(19), 2735-2741. http://dx.doi.org/10.1039/b409157d PMID: 15455144

[14] Xie, L.; Xie, L.; Kinnings, S.L.; Bourne, P.E. Novel computational approaches to polypharmacology as a means to define responses to individual drugs. **Annu. Rev. Pharmacol. Toxicol.**, **2012**, **52**, 361-379. http://dx.doi.org/10.1146/annurev-pharmtox-010611-134630 PMID: 22017683

[15] Hopkins, A.L. Network pharmacology: the next paradigm in drug discovery. **Nat. Chem. Biol.**, **2008**, **4**(11), 682-690. http://dx.doi.org/10.1038/nchembio.118 PMID: 18936753

[16] Lu, L.; Payvandi, F.; Wu, L.; Zhang, L.H.; Hariri, R.J.; Man, H.W.; Chen, R.S.; Muller, G.W.; Hughes, C.C.; Stirling, D.I.; Schafer, P.H.; Bartlett, J.B. The anti-cancer drug lenalidomide inhibits angiogenesis and metastasis via multiple inhibitory effects on endothelial cell function in normoxic and hypoxic conditions. **Microvasc. Res.**, **2009**, **77**(2), 78-86. http://dx.doi.org/10.1016/j.mvr.2008.08.003 PMID: 18805433

[17] Lindert, S.; Zhu, W.; Liu, Y.L.; Pang, R.; Oldfield, E.; McCammon, J.A. Farnesyl diphosphate synthase inhibitors from in silico screening. **Chem. Biol. Drug Des.**, **2013**, **81**(6), 742-748. http://dx.doi.org/10.1111/cbdd.12121 PMID: 23421555

[18] Zhu, W.; Zhang, Y.; Sinko, W.; Hensler, M.E.; Olson, J.; Molohon, K.J.; Lindert, S.; Cao, R.; Li, K.; Wang, K.; Wang, Y.; Liu, Y.L.; Sankovsky, A.; de Oliveira, C.A.; Mitchell, D.A.; Nizet, V.; McCammon, J.A.; Oldfield, E. Antibacterial drug leads targeting isoprenoid biosynthesis. **Proc. Natl. Acad. Sci. USA**, **2013**, **110**(1), 123-128. http://dx.doi.org/10.1073/pnas.1219899110 PMID: 23248302

[19] Leelananda, S.P.; Lindert, S. Computational methods in drug discovery. **Beilstein J. Org. Chem.**, **2016**, **12**, 2694-2718. http://dx.doi.org/10.3762/bjoc.12.267 PMID: 28144341

[20] Talele, T.T.; Khedkar, S.A.; Rigby, A.C. Successful applications of computer aided drug discovery: moving drugs from concept to the clinic. **Curr. Top. Med. Chem.**, **2010**, **10**(1), 127-141.

http://dx.doi.org/10.2174/156802610790232251 PMID: 19929824

[21] Clark, D.E. What has computer-aided molecular design ever done for drug discovery? **Expert Opin. Drug Discov.**, **2006**, **1**(2), 103-110.
http://dx.doi.org/10.1517/17460441.1.2.103 PMID: 23495794

[22] Friesner, R.A.; Banks, J.L.; Murphy, R.B.; Halgren, T.A.; Klicic, J.J.; Mainz, D.T.; Repasky, M.P.; Knoll, E.H.; Shelley, M.; Perry, J.K.; Shaw, D.E.; Francis, P.; Shenkin, P.S. Glide: a new approach for rapid, accurate docking and scoring. 1. Method and assessment of docking accuracy. **J. Med. Chem.**, **2004**, **47**(7), 1739-1749.
http://dx.doi.org/10.1021/jm0306430 PMID: 15027865

[23] McGann, M. FRED pose prediction and virtual screening accuracy. **J. Chem. Inf. Model.**, **2011**, **51**(3), 578-596.
http://dx.doi.org/10.1021/ci100436p PMID: 21323318

[24] Trott, O.; Olson, A.J. AutoDock Vina: improving the speed and accuracy of docking with a new scoring function, efficient optimization, and multithreading. **J. Comput. Chem.**, **2010**, **31**(2), 455-461.
PMID: 19499576

[25] Verdonk, M.L.; Cole, J.C.; Hartshorn, M.J.; Murray, C.W.; Taylor, R.D. Improved protein-ligand docking using GOLD. **Proteins**, **2003**, **52**(4), 609-623.
http://dx.doi.org/10.1002/prot.10465 PMID: 12910460

[26] Kramer, B.; Rarey, M.; Lengauer, T. Evaluation of the FLEXX incremental construction algorithm for protein-ligand docking. **Proteins**, **1999**, **37**(2), 228-241.
http://dx.doi.org/10.1002/(SICI)1097-0134(19991101)37:2<228::AID-PROT8>3.0.CO;2-8 PMID: 10584068

[27] Sinko, W.; Lindert, S.; McCammon, J.A. Accounting for receptor flexibility and enhanced sampling methods in computer-aided drug design. **Chem. Biol. Drug Des.**, **2013**, **81**(1), 41-49.
http://dx.doi.org/10.1111/cbdd.12051 PMID: 23253130

[28] Feixas, F.; Lindert, S.; Sinko, W.; McCammon, J.A. Exploring the role of receptor flexibility in structure-based drug discovery. **Biophys. Chem.**, **2014**, **186**, 31-45.
http://dx.doi.org/10.1016/j.bpc.2013.10.007 PMID: 24332165

[29] Feng, X.; Zhu, W.; Schurig-Briccio, L.A.; Lindert, S.; Shoen, C.; Hitchings, R.; Li, J.; Wang, Y.; Baig, N.; Zhou, T.; Kim, B.K.; Crick, D.C.; Cynamon, M.; McCammon, J.A.; Gennis, R.B.; Oldfield, E. Antiinfectives targeting enzymes and the proton motive force. **Proc. Natl. Acad. Sci. USA**, **2015**, **112**(51), E7073-E7082.
http://dx.doi.org/10.1073/pnas.1521988112 PMID: 26644565

[30] Kim, M.O.; Feng, X.; Feixas, F.; Zhu, W.; Lindert, S.; Bogue, S.; Sinko, W.; de Oliveira, C.; Rao, G.; Oldfield, E.; McCammon, J.A. A Molecular Dynamics Investigation of Mycobacterium tuberculosis Prenyl Synthases: Conformational Flexibility and Implications for Computer-aided Drug Discovery. **Chem. Biol. Drug Des.**, **2015**, **85**(6), 756-769.
http://dx.doi.org/10.1111/cbdd.12463 PMID: 25352216

[31] Zinsser, V.L.; Lindert, S.; Banford, S.; Hoey, E.M.; Trudgett, A.; Timson, D.J. UDP-galactose 4′-epimerase from the liver fluke, Fasciola hepatica: biochemical characterization of the enzyme and identification of inhibitors. **Parasitology**, **2015**, **142**(3), 463-472.
http://dx.doi.org/10.1017/S003118201400136X PMID: 25124392

[32] Banzo Marraco, J.I.; de la Fuente Domínguez, C.; Carril Carril, J.M.; Lloréns Abando, V.; Arnal Mendive, C.; Santos Capilla, J.L.; Pereda de la Reguera, A. [Usefulness of hepatobiliary gammagraphy in the diagnosis of biliary obstruction]. **Rev. Clin. Esp.**, **1986**, **179**(5), 236-239. [Usefulness of hepatobiliary gammagraphy in the diagnosis of biliary obstruction].
PMID: 3538244

[33] Barakat, K.; Tuszynski, J. Relaxed complex scheme suggests novel inhibitors for the lyase activity of DNA polymerase beta. **J. Mol. Graph. Model.**, **2011**, **29**(5), 702-716.
http://dx.doi.org/10.1016/j.jmgm.2010.12.003 PMID: 21194999

[34] Barakat, K.; Mane, J.; Friesen, D.; Tuszynski, J. Ensemble-based virtual screening reveals dual-inhibitors for the p53-MDM2/MDMX interactions. **J. Mol. Graph. Model.**, **2010**, **28**(6), 555-568.
http://dx.doi.org/10.1016/j.jmgm.2009.12.003 PMID: 20056466

[35] Barakat, K.H.; Torin Huzil, J.; Luchko, T.; Jordheim, L.; Dumontet, C.; Tuszynski, J. Characterization of an inhibitory dynamic pharmacophore for the ERCC1-XPA interaction using a combined molecular dynamics and virtual screening approach. **J. Mol. Graph. Model.**, **2009**, **28**(2), 113-130.
http://dx.doi.org/10.1016/j.jmgm.2009.04.009 PMID: 19473860

[36] Lindert, S.; Meiler, J.; McCammon, J.A. Iterative Molecular Dynamics-Rosetta Protein Structure Refinement Protocol to Improve Model Quality. **J. Chem. Theory Comput.**, **2013**, **9**(8), 3843-3847.
http://dx.doi.org/10.1021/ct400260c PMID: 23956701

[37] Lindert, S.; Li, M.X.; Sykes, B.D.; McCammon, J.A. Computer-aided drug discovery approach finds calcium sensitizer of cardiac troponin. **Chem. Biol. Drug Des.**, **2015**, **85**(2), 99-106.
http://dx.doi.org/10.1111/cbdd.12381 PMID: 24954187

[38] Lindert, S.; Cheng, Y.; Kekenes-Huskey, P.; Regnier, M.; McCammon, J.A. Effects of HCM cTnI mutation R145G on troponin structure and modulation by PKA phosphorylation elucidated by molecular dynamics simulations. **Biophys. J.**, **2015**, **108**(2), 395-407.
http://dx.doi.org/10.1016/j.bpj.2014.11.3461 PMID: 25606687

[39] Liu, Y.L.; Lindert, S.; Zhu, W.; Wang, K.; McCammon, J.A.; Oldfield, E. Taxodione and arenarone inhibit farnesyl diphosphate synthase by binding to the isopentenyl diphosphate site. **Proc. Natl. Acad. Sci. USA**, **2014**, **111**(25), E2530-E2539.
http://dx.doi.org/10.1073/pnas.1409061111 PMID: 24927548

[40] Menchon, G.; Bombarde, O.; Trivedi, M.; Négrel, A.; Inard, C.; Giudetti, B.; Baltas, M.; Milon, A.; Modesti, M.; Czaplicki, G.; Calsou, P. Structure-Based Virtual Ligand Screening on the XRCC4/DNA Ligase IV Interface. **Sci. Rep.**, **2016**, **6**, 22878.
http://dx.doi.org/10.1038/srep22878 PMID: 26964677

[41] Wong, C.F. Conformational transition paths harbor structures useful for aiding drug discovery and understanding enzymatic mechanisms in protein kinases. **Protein Sci.**, **2016**, **25**(1), 192-203.
http://dx.doi.org/10.1002/pro.2716 PMID: 26032746

[42] Bhutani, I.; Loharch, S.; Gupta, P.; Madathil, R.; Parkesh, R. Structure, dynamics, and interaction of Mycobacterium tuberculosis (Mtb) DprE1 and DprE2 examined by molecular modeling, simulation, and electrostatic studies. **PLoS One**, **2015**, **10**(3)e0119771
http://dx.doi.org/10.1371/journal.pone.0119771 PMID: 25789990

[43] Aprahamian, M.L.; Tikunova, S.B.; Price, M.V.; Cuesta, A.F.; Davis, J.P.; Lindert, S. Successful Identification of Cardiac Troponin Calcium Sensitizers Using a Combination of Virtual Screening and ROC Analysis of Known Troponin C Binders. **J. Chem. Inf. Model.**, **2017**, **57**(12), 3056-3069.
http://dx.doi.org/10.1021/acs.jcim.7b00536 PMID: 29144742

[44] Lindert, S.; Tallorin, L.; Nguyen, Q.G.; Burkart, M.D.; McCammon, J.A. In silico screening for Plasmodium falciparum enoyl-ACP reductase inhibitors. **J. Comput. Aided Mol. Des.**, **2015**, **29**(1), 79-87.
http://dx.doi.org/10.1007/s10822-014-9806-3 PMID: 25344312

[45] Lindert, S.; Maslennikov, I.; Chiu, E.J.; Pierce, L.C.; McCammon, J.A.; Choe, S. Drug screening strategy for human membrane proteins: from NMR protein backbone structure to in silica- and NMR-screened hits. **Biochem. Biophys. Res. Commun.**, **2014**, **445**(4), 724-733.
http://dx.doi.org/10.1016/j.bbrc.2014.01.179 PMID: 24525125

[46] Tutone, M.; Almerico, A.M. Recent advances on CDK inhibitors: An insight by means of in silico methods. **Eur. J. Med. Chem.**, **2017**, **142**, 300-315.
http://dx.doi.org/10.1016/j.ejmech.2017.07.067 PMID: 28802482

[47] Martin, M.P.; Endicott, J.A.; Noble, M.E.M. Structure-based discovery of cyclin-dependent protein kinase inhibitors. **Essays Biochem.**, **2017**, **61**(5), 439-452.
http://dx.doi.org/10.1042/EBC20170040 PMID: 29118092

[48] Hernandez, M.; Ghersi, D.; Sanchez, R. SITEHOUND-web: a server for ligand binding site identification in protein structures. **Nucleic Acids Res**, **2009**, **37** (Web Server issue), W413-6
http://dx.doi.org/10.1093/nar/gkp281

[49] National Cancer Institute. NIH: Division of Cancer Treatment & Diagnosis. Developmental Therapeutics Program. . http://dtp.nci.nih.gov/branches/dscb/div2_explanation.html

[50] MacKerell, A.D.; Bashford, D.; Bellott, M.; Dunbrack, R.L.; Evanseck, J.D.; Field, M.J.; Fischer, S.; Gao, J.; Guo, H.; Ha, S.; Joseph-McCarthy, D.; Kuchnir, L.; Kuczera, K.; Lau, F.T.; Mattos, C.; Michnick, S.; Ngo, T.; Nguyen, D.T.; Prodhom, B.; Reiher, W.E.; Roux, B.; Schlenkrich, M.; Smith, J.C.; Stote, R.; Straub, J.; Watanabe, M.; Wiórkiewicz-Kuczera, J.; Yin, D.; Karplus, M. All-

atom empirical potential for molecular modeling and dynamics studies of proteins. **J. Phys. Chem. B**, **1998**, **102**(18), 3586-3616. http://dx.doi.org/10.1021/jp973084f PMID: 24889800

[51] Durrant, J.D.; Votapka, L.; Sørensen, J.; Amaro, R.E. POVME 2.0: An Enhanced Tool for Determining Pocket Shape and Volume Characteristics. **J. Chem. Theory Comput.**, **2014**, **10**(11), 5047-5056. http://dx.doi.org/10.1021/ct500381c PMID: 25400521

[52] Christen, M.; Hünenberger, P.H.; Bakowies, D.; Baron, R.; Bürgi, R.; Geerke, D.P.; Heinz, T.N.; Kastenholz, M.A.; Kräutler, V.; Oostenbrink, C.; Peter, C.; Trzesniak, D.; van Gunsteren, W.F. The GROMOS software for biomolecular simulation: GROMOS05. **J. Comput. Chem.**, **2005**, **26**(16), 1719-1751. http://dx.doi.org/10.1002/jcc.20303 PMID: 16211540

[53] Dahlin, J.L.; Nissink, J.W.; Strasser, J.M.; Francis, S.; Higgins, L.; Zhou, H.; Zhang, Z.; Walters, M.A. PAINS in the assay: chemical mechanisms of assay interference and promiscuous enzymatic inhibition observed during a sulfhydryl-scavenging HTS. **J. Med. Chem.**, **2015**, **58**(5), 2091-2113. http://dx.doi.org/10.1021/jm5019093 PMID: 25634295

[54] Baell, J.B.; Holloway, G.A. New substructure filters for removal of pan assay interference compounds (PAINS) from screening libraries and for their exclusion in bioassays. **J. Med. Chem.**, **2010**, **53**(7), 2719-2740. http://dx.doi.org/10.1021/jm901137j PMID: 20131845

[55] Kenyon, V.; Chorny, I.; Carvajal, W.J.; Holman, T.R.; Jacobson, M.P. Novel human lipoxygenase inhibitors discovered using virtual screening with homology models. **J. Med. Chem.**, **2006**, **49**(4), 1356-1363. http://dx.doi.org/10.1021/jm050639j PMID: 16480270

[56] Kim, S.S.; Aprahamian, M.L.; Lindert, S. Improving inverse docking target identification with Z-score selection. **Chem. Biol. Drug Des.**, **2019**, **93**(6), 1105-1116. http://dx.doi.org/10.1111/cbdd.13453 PMID: 30604454

[57] Feher, M. Consensus scoring for protein-ligand interactions. **Drug Discov. Today**, **2006**, **11**(9-10), 421-428. http://dx.doi.org/10.1016/j.drudis.2006.03.009 PMID: 16635804

[58] Clark, R.D.; Strizhev, A.; Leonard, J.M.; Blake, J.F.; Matthew, J.B. Consensus scoring for ligand/protein interactions. **J. Mol. Graph. Model.**, **2002**, **20**(4), 281-295. http://dx.doi.org/10.1016/S1093-3263(01)00125-5 PMID: 11858637

[59] Oda, A.; Tsuchida, K.; Takakura, T.; Yamaotsu, N.; Hirono, S. Comparison of consensus scoring strategies for evaluating computational models of protein-ligand complexes. **J. Chem. Inf. Model.**, **2006**, **46**(1), 380-391. http://dx.doi.org/10.1021/ci050283k PMID: 16426072

[60] Charifson, P.S.; Corkery, J.J.; Murcko, M.A.; Walters, W.P. Consensus scoring: A method for obtaining improved hit rates from docking databases of three-dimensional structures into proteins. **J. Med. Chem.**, **1999**, **42**(25), 5100-5109. http://dx.doi.org/10.1021/jm990352k PMID: 10602695

[61] Martin, Y.C.; Kofron, J.L.; Traphagen, L.M. Do structurally similar molecules have similar biological activity? **J. Med. Chem.**, **2002**, **45**(19), 4350-4358. http://dx.doi.org/10.1021/jm020155c PMID: 12213076

[62] **1987**. http://osc.edu/ark:/19495/f5s1ph73